Supplementary material

Metabolic activation of myristicin and its role in cellular toxicity

Xu Zhu[a,b,†], Yi-Kun Wang[a,b,†], Xiao-Nan Yang[a,c], Xue-Rong Xiao[a], Ting Zhang[a,b], Xiu-Wei Yang[d], Hong-Bo Qin[a], Fei Li[a,e]

[a]States Key Laboratory of Phytochemistry and Plant Resources in West China, Kunming Institute of Botany, Chinese Academy of Sciences, Kunming 650201, China

[b]University of Chinese Academy of Sciences, Beijing 100049, China

[c]Guangxi Key Laboratory of Medicinal Resources Protection and Genetic Improvement, Guangxi Botanical Garden of Medicinal Plant, Nanning 530023, China

[d]School of Pharmaceutical Sciences, Peking University Health Science Center, Peking University, Beijing 100191, China

[e]Jiangxi University of Traditional Chinese Medicine, Nanchang 330004, China

Chemical syntheses of 1'-hydroxymyristicin

The synthesis of 1'-hydroxymyristicin was completed by Professor Hong-bo Qin's laboratory. 1'-Hydroxymyristicin was synthesized using nucleophilic addition of 5-Methoxypiperonal. To a solution of 5-methoxypiperonal (101 mg, 0.56 mmol) in anhydrous tetrahydrofuran (2 mL) under N_2 was supplemented Vinylmagnesium bromide (0.56 mL, 1 mol/L, 0.56 mmol) dropwise at 0 ℃. After being stirred for 1h at 25 ℃, the mixture was terminated by saturated aqueous NH_4Cl and extracted with ethyl acetate (EtOAc) three times. Combined organic phase was washed sequentially with saturated aqueous sodium carbonate solution, water and brine, and dried over Na_2SO_4. Filtration and concentration afforded the crude product. Purification by column chromatography using EtOAc/Petroleum ether (1:10) as mobile phase gave alcohol product (96 mg, 82%) as a colorless oil. The purity of 1'-hydroxymyristicin was > 98% measured by high-performance liquid chromatography. NMR spectra data were operated on 600 MHz for ^{1}H-NMR spectrum and 150 MHz for ^{13}C-NMR spectral. Deuterochloroform ($CDCl_3$) was used as solvents for NMR detection. The structural identification of 1'-hydroxymyristicin was characterized by ^{1}H- and ^{13}C-NMR spectral (Supplementary Fig. 1A and 1B). ^{1}H-NMR ($CDCl_3$, 600 MHz): δ 3.88 (3H, s, OCH_3), 5.93 (2H, s, -OCH_2O-), 6.55 (1H, s, 2-H), 6.53 (1H, s, 4-H), 5.32 (1H, d, H1'), 5.97 (1H, d, H2'), 5.16/5.05 (2H, d, CH_2=) (Supplementary Fig.1A). ^{13}C-NMR ($CDCl_3$, 150MHz): δ 143.53 (C-1), 134.53 (C-2), 148.83 (C-3), 101.42 (C-4), 137.52 (C-5), 100.59 (C-6), 75.08 (C-1'), 140.13 (C-2'), 114.52 (C-3'), 56.50 (-OCH_3), 105.70 (-OCH_2O-) (Supplementary Fig.1B). HR-ESI-MS: *m/z*

231.0633 $[M+Na]^+$ (calculated for $C_{11}H_{12}O_4$).

Sample preparation method of urine, feces and blood

For urine samples preparation, 180 μL of 50% aqueous acetonitrile containing 5 μM of chlorpropamide (used as internal standard) was added into 20 μL of urine sample, and vortexed for 1 min. Then the samples were centrifuged at 18000 *g* for 20 min at 4 ℃ to remove proteins and particulates. For plasma samples preparation, 190 μL of 50% aqueous acetonitrile containing 5 μM of chlorpropamide (used as internal standard) was added into 10 μL of plasma sample, and vortexed for 1 min. Then the samples were centrifuged at 18 000 *g* for 20 min at 4 ℃ to remove proteins and particulates. For feces samples preparation, 20 mg of each feces sample was homogenized with 10-fold of 50% aqueous acetonitrile (containing 5 uM chlorpropamide), shaken for 20 min at room temperature. Then the samples were centrifuged at 18000 *g* for 20 min at 4 ℃. After that, 100 μL of each supernatant was transferred to new tube. Then 200 μL of 50% aqueous acetonitrile was added into each sample. The diluted samples were again centrifuged at 18000 *g* for 20 min at 4 ℃. The supernatants were transferred to new tubes and 5 μL aliquot of each sample was injected for UPLC-ESI-QTOFMS analysis.

Structural identification of 1'-hydroxymyristicin and its metabolites

The chromatic pattern and fragment pathway of **H0** were consistent with

1'-hydroxymyristicin (Supplementary Fig. 5A). Metabolite **H1** was detected at *m/z* 209.0808 in full scan mode of MLMs sample at t_R of 8.42 min, which matched structural formula of $C_{11}H_{12}O_4$. It was similar to **H0**, demonstrating that **H1** may be isomerization product of 1'-hydroxymyristicin. Different from the fragment pathway of 1'-hydroxymyristicin, **H1** gave various daughter ions included *m/z* 193.0555 (loss of O atom), 179.0677 (loss of CH_2O moiety), 165.0522 (loss of CH_2O+CH_2 moiety) and 137.0928, which implied **H1** was hydroxyl isomerization product at site of ally (Supplementary Fig. 5B). The retention time and fragments of metabolite **H2** were consistent with **M6**, suggesting that **H2** and **M6** were the same metabolites from myristicin and 1'-hydroxymyristicin metabolism, respectively. The MS/MS spectrum of metabolite **H3** revealed a molecular ion $[M+H]^+$ of *m/z* 179.0703, and was 30 Da (OCH_2) higher than parents, demonstrating that **H3** may be demethoxylated 1'-hydroxymyristicin. Fragmentation of its molecular ion resulted in ions at *m/z* 161, 137, through neutral loss of 18 Da (H_2O) and 42 Da (C_2H_2 +O).

Metabolite **H5** yielded $[M+H]^+$ at *m/z* 225.0757, and fragments of *m/z* 207 (dehydration), 184 $[(M+H)\text{-}CO\text{-}CH_2]^+$ and 165 (6-vinylbenzo[d][1,3]dioxol-4-ol residue) were observed in the MS/MS spectrum. The characteristic ion of *m/z* 184 (7-methoxybenzo[d][1,3]dioxol-5-yl)methanol) was formed via neutral losses of acetaldehyde in the site of chain, suggesting **H5** was 3-hydroxy-3-(7-methoxybenzo[d][1,3]dioxol-5-yl)propanal. Metabolite **H4** (t_R = 6.94 min, observed $[M+H]^+$ at *m/z* 223.0601) gave a match for the molecular formula $C_{11}H_{10}O_5$, and was 2 Da (H_2) lower than **H5**, suggesting **H4** was dehydrogenated product of **H5**.

According to the major two related fragment ions of **H4** at *m/z* 205 $[M+H-H_2O]^+$, 165^+ (6-vinylbenzo[d][1,3]dioxol-4-ol residue), it was identified **H4** as 2',3'-dicarbonylated myristicin. Metabolite **H6** exhibited an abundant parent ion $[M+H]^+$ at *m/z* 207.0652, which accurately matched $C_{11}H_{10}O_4$,. It was 2 Da (H_2) lower than parent, implying that **H6** was dehydrogenated product via hydroxyl oxidation. Two daughter ions of **H6** at *m/z* 177 $[M+H-CH_2O]^+$ and 149 $[M+H-(CH_2O+CO)]^+$ were observed on the MS^2 spectra. Metabolite **H7** exhibited quasi-molecular $[M+H]^+$ ion at *m/z* 195.0662, which gave a match for the molecular formula of $C_{10}H_{10}O_4$ with the error of -5.15 ppm. It was lower 14 Da than parent, suggesting that **H7** was demethylated 1'-hydroxymyristicin. **H7** yielded the major daughter ions at *m/z* 153 (cleavage of CH_2=CH-OH), and 123 (cleavage of CH_2=CH-CHOH+O) (Supplementary Fig. 5C).

The structural formula of **H8** was speculated as $C_9H_8O_4$ from protonated molecular $[M+H]^+$ ion at *m/z* 181.0495. It was lower 28 Da (CH_2=CH_2) than 1'-hydroxymyristicin, implying that **H8** was devinylated 1'-hydroxymyristicin. It produced prominent fragment ions at *m/z* 153 (cleavage of CH_2=CH-OH), and 123 (cleavage of CH_2=CH-CHOH+O). The chromatic pattern and fragment pathways of **H9** were consistent with **M3**. The daughter ion spectra of **H10** showed the diagnostic neutral loss of 101 Da (*m/z* 328→207), indicating the presence of a cysteine moiety via the linker of sulfur atom. Furthermore, protonated cysteine ion *m/z* at 122 was discovered in MS/MS spectrum of **H10.** Thereby, **H10** was characterized as 1'-hydroxymyristicin plus cysteine conjugate (Supplementary Fig. 5D).

Figure Captions

Supplementary Fig. 1 NMR spectral of 1'-hydroxymyristicin. (A) ^{1}H-NMR spectrum of 1'-hydroxymyristicin. (B) ^{13}C-NMR spectrum of 1'-hydroxymyristicin.

Supplementary Fig. 2 The relative abundance of myristicin and its metabolites in urine (A), in plasma (B) and in microsomes (C).

Supplementary Fig. 3 The relative abundance of 1'-hydroxymyristicin and its metabolites in urine (A), in plasma (B) and in microsomes (C).

Supplementary Fig. 4 MS^2 spectrums and fragmentation pathways of **M0** (A), **M1** (B), **M2** (C) and **M6** (D).

Supplementary Fig. 5 MS^2 spectrums and fragmentation pathways of **H0** (A), **H1** (B), **H7** (C) and **H10** (D).

Supplementary Table1. Summary of metabolites of myristicin produced *in vivo* and *in vitro* metabolism

Metabolits (ID)	*R*t (min)	Observed $[M+H]^+$	Molecular formula	Mass error (ppm)	Major fragment ions	Reaction	Identity	Source
M0	9.95	193.0859	$C_{11}H_{12}O_3$	0.43	163,152,135	-	Myristicin	M,H,U,P
M1*	6.12	195.0973	$C_{11}H_{14}O_3$	-5.15	181,165	1	2',3'-Reduced-myristicin	M,H,U
M2*	5.97	179.0683	$C_{10}H_{10}O_3$	7.39	161,151,147	2	3-Hydroxysafrole	M,H,U
M3	6.02	227.0903	$C_{11}H_{14}O_5$	7.59	167,109,81	3	2',3'-Dihydroxy myristicin	M,H,U
M4	5.99	209.0812	$C_{11}H_{12}O_4$	-8.02	179,168,94	4	4-or 6-Hydroxy myristicin	M,H,U
M5	6.61	181.0862	$C_{10}H_{12}O_3$	2.76	154,135,121	5	5-Allyl-1-methoxy-2,3-dihydroxybenzene	M,H,U
M6*	5.54	191.0686	$C_{11}H_{10}O_3$	7.85	161,133	6	2',3'-Dehydro-myristicin	M,H,U
M7*	5.62	165.0552	$C_9H_8O_3$	-2.27	131,115	7	4-Allyl-2-methoxyphenol	M,H
M8	6.87	231.0633Na^+	$C_{11}H_{12}O_4$	-4.33	213,191,165	4	1'-Hydroxymyristicin	M,H
M9	5.97	385.1092	$C_{17}H_{20}O_{10}$	5.52	209,165,147	4+Gluc	Myristicin-Gluc adduct	U
M10*	6.39	370.0947	$C_{16}H_{19}NS_7$	-1.62	207,164,122	4+ NAC	Myristicin-NAC adduct	U

1, Reduction; 2, Demethylation; 3, Alkenes to dihydrodiol; 4, Hydroxylation; 5, open-ring; 6, Desaturation; 7, Demethylation; Gluc, glucuronide; NAC, *N*-acetylcysteine; U, urine; P, plasma; M, mouse liver microsomes; H, human liver microsomes. *****Indicate novel metabolites found in this study.

Supplementary Table 2. Summary of metabolites of 1'-hydroxymyristicin produced *in vivo* and *in vitro* metabolism

Metabolites (ID)	*R*t (min)	Observed $[M+H]^+$	Molecular formula	Mass error (ppm)	Major fragment ions	Reaction	Identity	Source
H0	6.87	231.0633Na^+	$C_{11}H_{12}O_4$	0.67	213,191,165,123	-	1'-Hydroxymyristicin	M, H, P
H1	8.42	209.0808	$C_{11}H_{12}O_4$	1.76	193,179,165,137	-	3'-Hydroxymyristicin	M,H,U
H2*	5.55	191.0682	$C_{11}H_{10}O_3$	1.17	161,133,97,69	1	2',3'-Dehydro-myristicin	M,H,P,U
H3*	6.28	179.0703	$C_{10}H_{10}O_3$	1.30	161,137	2	Demethoxy -1'-hydroxymyristicin	M, H
H4*	6.94	223.0601	$C_{11}H_{10}O_5$	7.63	205,165	3	1'3'-Dioxo-myristicin	M,H,P
H5*	6.73	225.0757	$C_{11}H_{12}O_5$	3.34	207,184,165	4	1'-Hydro-3'-oxo-mxymyristicin	P
H6*	5.74	207.0652	$C_{11}H_{10}O_4$	0.56	177,149,81	5	1'-Oxo-mxymyristicin	P
H7*	7.27	195.0662	$C_{10}H_{10}O_4$	-3.97	153,123	6	Dimethyl-myristicin	U
H8*	6.99	181.0495	$C_9H_8O_4$	-5.15	153.123,93	7	Myristic aldehyde	U
H9	6.02	227.0942	$C_{11}H_{14}O_5$	-2.97	167,109,81	8	1'3'-Dihydroxymyristicin	U
H10*	5.02	328.0862	$C_{14}H_{17}NS_6$	-0.23	207,122,85,55	**H0**+ *S*-Cys	Hydroxymyristicin-Cys adduct	U
H11*	6.40	370.0952	$C_{16}H_{19}NS_7$	-0.74	207,164,122,55	**H0**+ NACys	Myristicin-NAC adduct	U

1, Alcohols dehydration; 2, hydroxymethylene loss; 3, Hydroxylation+desaturation; 4, Hydroxylation; 5, desaturation; 6, Demethylation; 7, Deethylation; 8, hydration; S-Cys, cysteine; NAC, acetylcysteine; U, urine; P, plasma; M, mouse liver microsomes; H, human liver microsomes.
*****Indicate novel metabolites found in this study.

Supplementary Table 3. Role of CYP450s in the formation of myristicin metabolites

No.	Enzyme	M1	M2	M3	M4	M5	M6	M7	M8
0	**Control**	-	-	-	-	-	-	-	-
1	**CYP1A1**	-	36.49	17.25	30.64	8.99	42.73	38.78	47.48
2	**CYP1A2**	29.27	-	-	-	47.69	10.99	-	-
3	**CYP1B1**	20.15	63.51	-	18.89	-	16.52	61.21	13.65
4	**CYP2A6**	-	-	17.75	-	-	9.28	-	-
5	**CYP2B6**	-	-	-	-	-	-	-	-
6	**CYP2C19**	-	-	-	-	-	-	-	-
7	**CYP2C8**	-	-	-	-	-	-	-	-
8	**CYP2C9**	-	-	27.04	-	-	-	-	21.82
9	**CYP2D6**	10.19	-	-	-	-	-	-	-
10	**CYP2E1**	-	-	-	-	-	-	-	-
11	**CYP3A4**	16.75	-	17.02	17.60	43.31	5.09	-	-
12	**CYP3A5**	23.62	-	20.93	32.86	-	15.38	-	17.05

cDNA-expressed CYPs (control, CYP1A1, 1A2, 1B1, 2A6, 2B6, 2C19, 2C8, 2C9, 2D6, 2E1, 3A4, 3A5, and 4A11) were used to examine the roles of in individual CYPs in myristicin metabolism. All samples were analyzed by UPLC-ESI-QTOF-MS. The total peak areas of each metabolites of myristicin form all the CYPs were set as 100%. All data are expressed as mean (n=3).

Supplementary Fig. 1

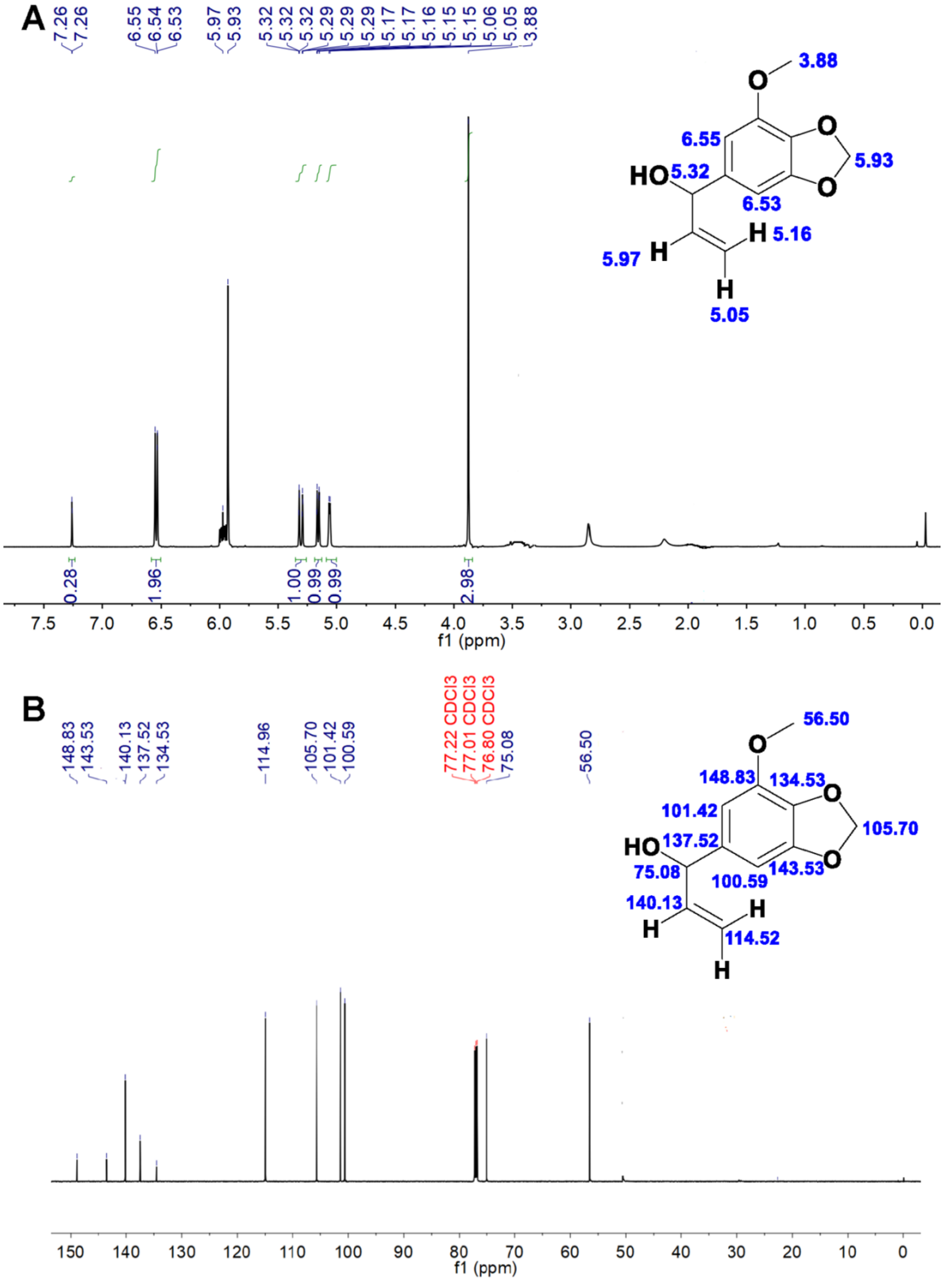

Supplementary Fig. 2

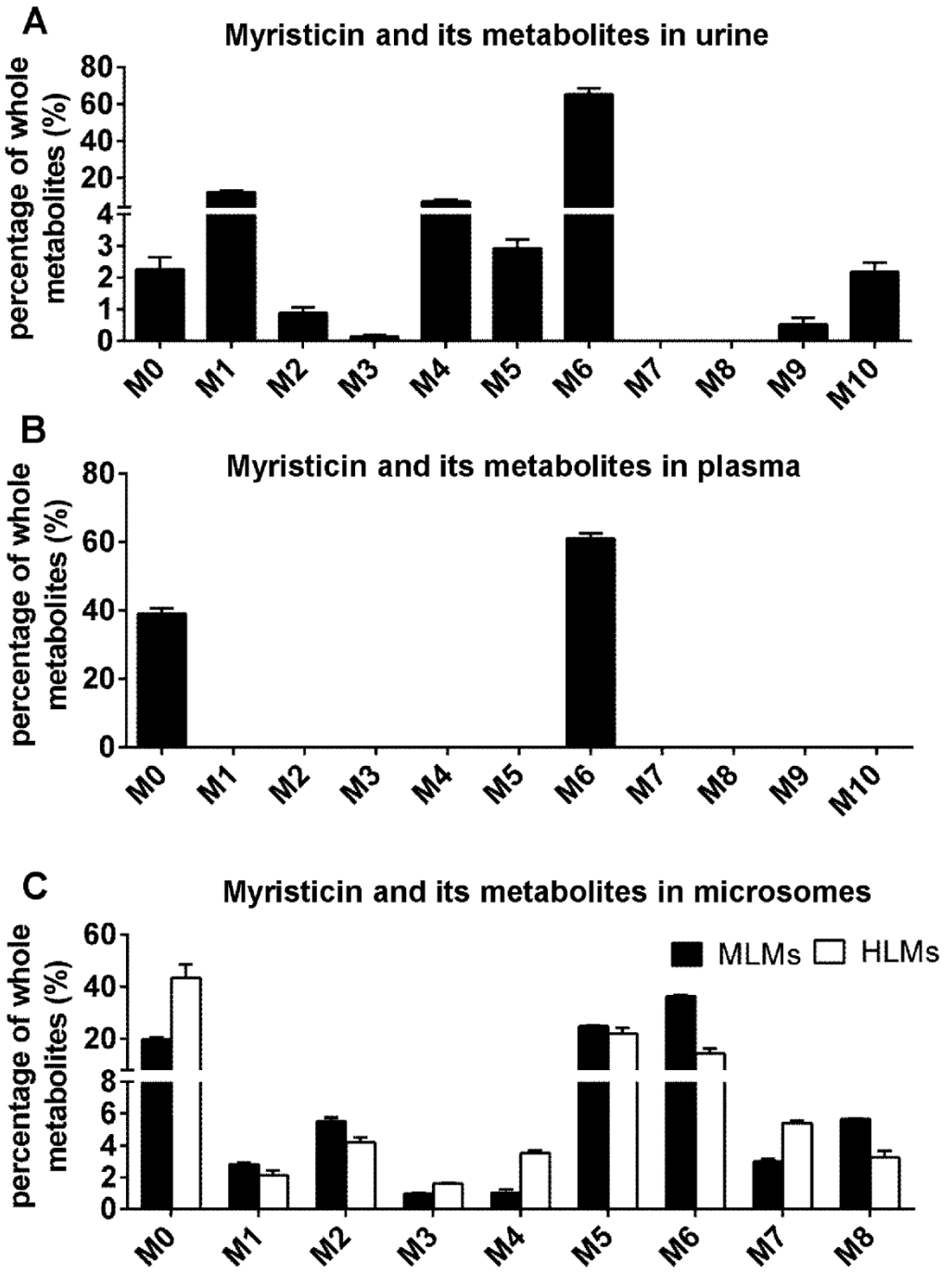

Supplementary Fig. 3

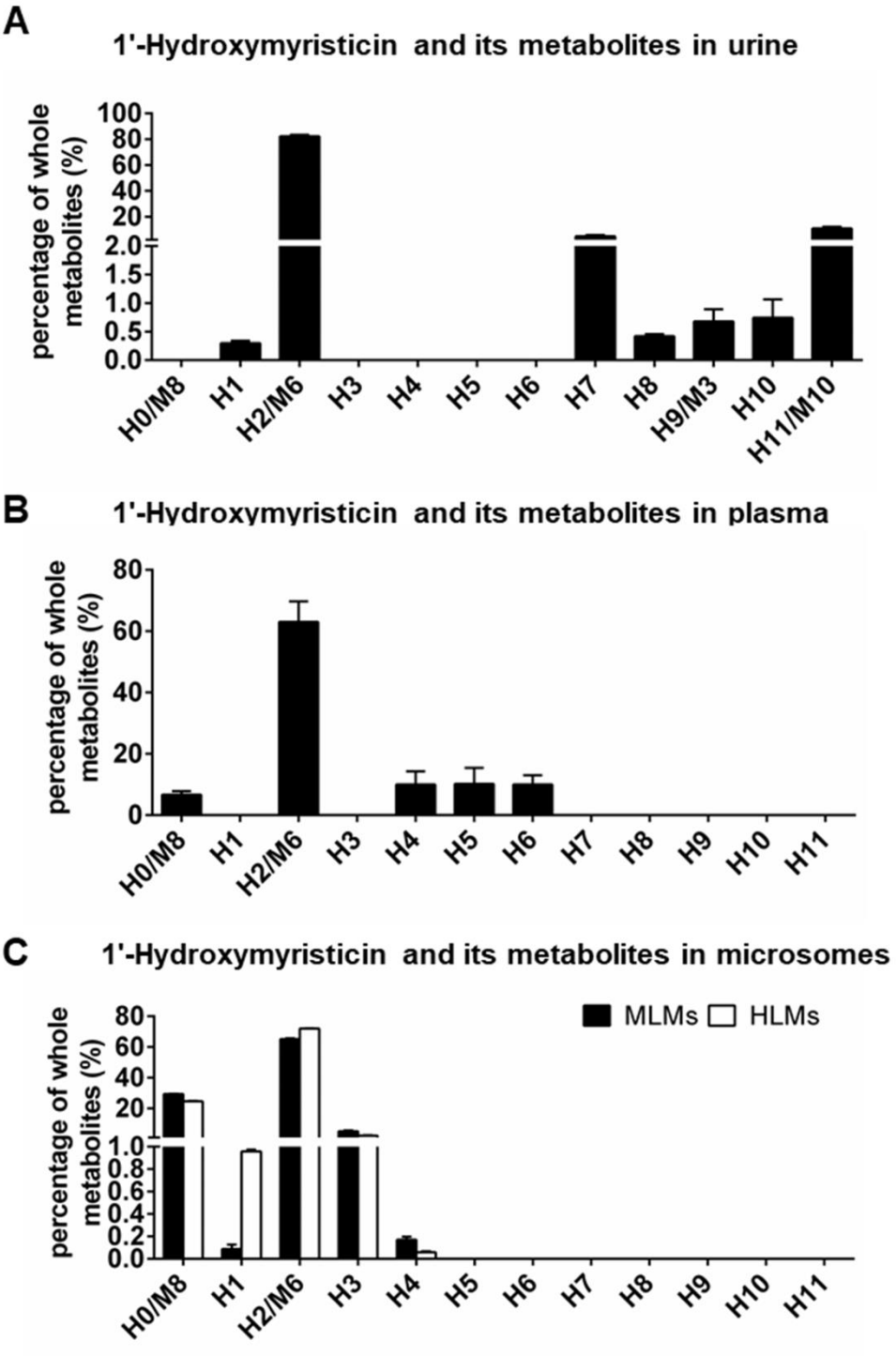

Supplementary Fig. 4

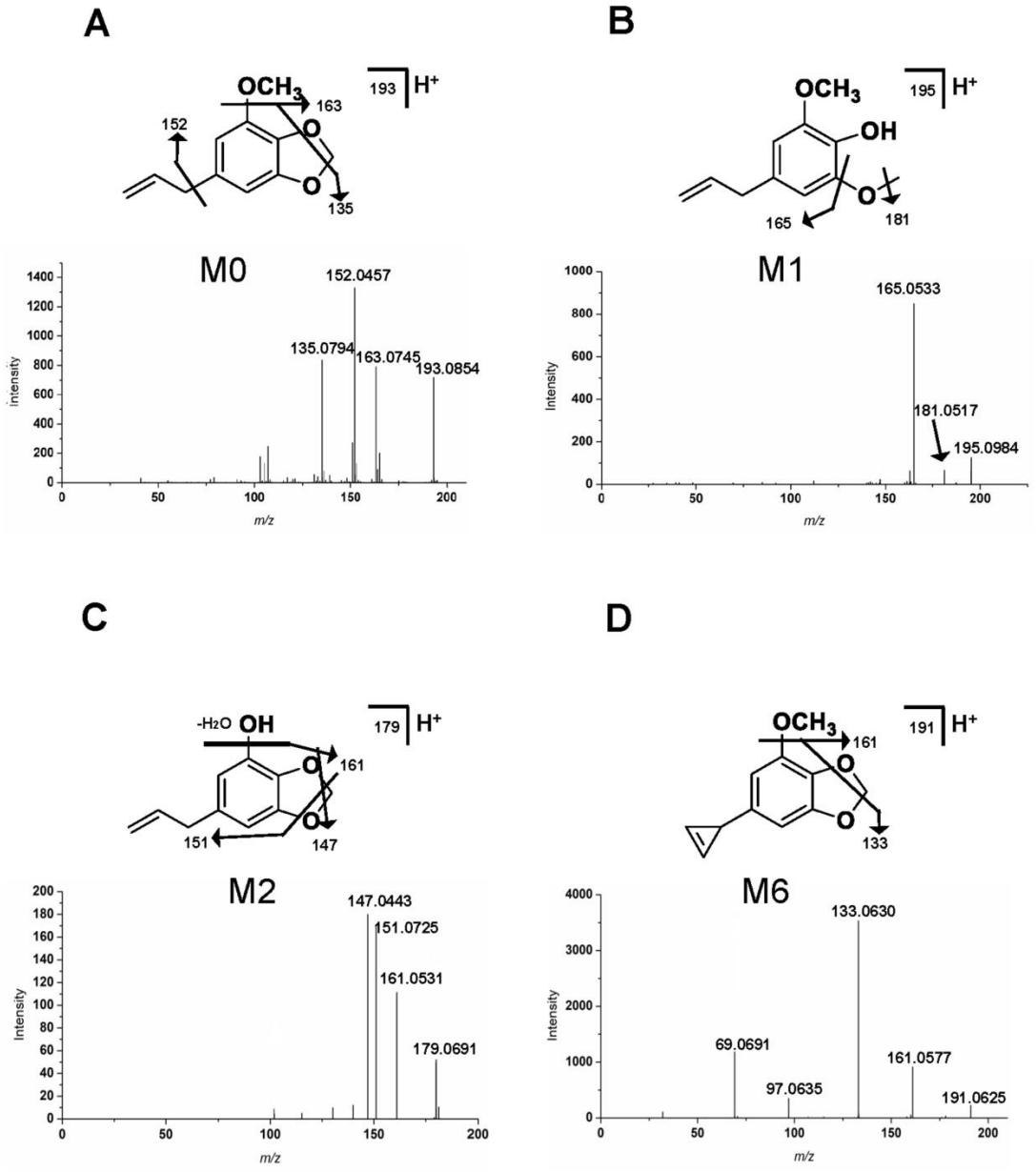

Supplementary Fig. 5